

Research Paper

Inhibition of STAT3 signaling as critical molecular event in HUC-MSCs suppressed Glioblastoma Cells

Mingming Wang^{1#}, Yufu Zhang^{2#}, Min Liu^{3#}, Yuna Jia¹, Jing He⁴, Xiangrong Xu¹, Haiyan Shi¹, Yunqing Zhang⁴, Jing Zhang¹, Yusi Liu¹

1. Department of Cell Biology and Genetics, Medical College of Yan'an University, Yan'an 716000, Shaanxi Province, China
2. Department of Hepatobiliary Surgery, Affiliated Hospital of Yan'an University, Yan'an 716000, Shaanxi Province, China
3. Department of Pathology, Affiliated Hospital of Yan'an University, Yan'an 716000, Shaanxi Province, China
4. Laboratory of Obstetrics and Gynecology, Affiliated Hospital of Yan'an University, Yan'an, 716000 Shaanxi Province, China

#These authors equally contributed to the paper.

 Corresponding authors: Yusi Liu, Department of Cell Biology and Genetics, Medical College of Yan'an University, Yan'an 716000, Shaanxi Province, China; E-mail addresses: zhangyq2881123@163.com (Y. Zhang), yadxzj@yau.edu.cn (J. Zhang), lys910615@163.com (Y. Liu), Tel: +86-0911-2332662

© The author(s). This is an open access article distributed under the terms of the Creative Commons Attribution License (<https://creativecommons.org/licenses/by/4.0/>). See <http://ivyspring.com/terms> for full terms and conditions.

Received: 2022.08.10; Accepted: 2023.01.17; Published: 2023.02.27

Abstract

Objective: We investigated the effect of human umbilical cord mesenchymal stem cells (HUC-MSCs) supernatants on proliferation, migration, invasion, and apoptosis in glioblastoma (GBM) cell lines RG-2, U251, U87-MG, and LN-428, as well as their apoptosis and autophagy-mediated through IL-6/JAK2/STAT3 signaling pathway to explore the molecular mechanisms.

Methods: In this study, RG-2, U251, U87-MG, and LN-428 cells were treated with 9 mg/ml HUC-MSCs supernatants. Their responses to HUC-MSCs supernatants treatment and the status of STAT3 signaling were analyzed by multiple experimental approaches to elucidate the importance of HUC-MSCs supernatants for GBM.

Results: The results demonstrated that after treatment with HUC-MSCs supernatants, *in vitro* proliferation of RG-2, U251, U87-MG, and LN-428 cells were inhibited, and their sustained growth was also blocked. RG-2, U251, and U87-MG cells showed significant S phase accumulation, while LN-428 cells were blocked in G0/G1 phase. Their migratory invasive capacities were inhibited, and their apoptosis and autophagy ratios were increased. These effects were mediated through the IL-6/JAK2/STAT3 and its downstream signaling pathway.

Conclusion: Our data showed that HUC-MSCs supernatants had anti-tumor effects on GBM cells. It inhibited the proliferation, migration, and invasion of GBM cells and promoted their apoptosis. Negative regulation of the IL-6/JAK2/STAT3 signaling pathway enhanced apoptosis and autophagy in tumor cells, thereby improving the therapeutic effect on GBM.

Keywords: human umbilical cord mesenchymal stem cell supernatant; glioblastoma; IL-6/JAK2/STAT3 signaling pathway

Introduction

Glioblastoma (GBM) is a primary brain tumor of the central nervous system in adults. It has been well-recognized that GBM was initiated by a subpopulation of cells termed glioblastoma stem cells (GSCs) [1, 2]. Central nervous system (CNS) gliomas are classified into 4 grades according to the WHO classification. WHO grades 1-2 are classified as low-grade gliomas (LGG), whereas WHO grades 3-4 are classified as high-grade gliomas (HGG) [3, 4]. The

incidence of LGG is low, and the prognosis is usually good [5]. GBM represents a grade 4 glioma. GBM is one of the most lethal and recurrent malignant solid tumors, accounting for 57% of all gliomas and 48% of primary CNS malignancies [6]. The median survival of patients with GBM is only 14.6 months. Currently, conventional treatment includes neurosurgery, temozolomide (TMZ) dependent chemotherapy [1, 2], and chemotherapy. Although GBM cells rarely

metastasize to other body organs, the treatment of GBM remains ineffective. The main reason for the poor prognosis of GBM is that conventional surgical resection often fails to eliminate the tumor, and the remaining tumor is often resistant to radiotherapy and chemotherapy, which inevitably leads to the recurrence of GBM [7]. The main reason for this problem is that many anti-GBM drugs cause significant toxicity to the brain and/or body at high doses. Another bottleneck that makes treatment tricky is the obstruction of the blood-brain barrier (BBB), this structure is essential for protecting a healthy brain and preventing the transport of toxic substances in the blood [8-11], which also hinders progress toward effective treatment of GBM [12]. However, it also impairs the ability of drugs to enter the brain for the effective treatment of lesions. It is the presence of these barriers that makes it difficult for many drugs to achieve the desired therapeutic efficacy. Therefore, there is an urgent need for a more effective strategy for treating GBM to complement or replace existing regimens.

Human umbilical cord mesenchymal stem cells (HUC-MSCs) possess multipotential differentiation abilities and self-renewal, and they are the most reliable source of stem cells in various cell therapies. Because of their multi-differentiation potential, high proliferation capacity, immune regulation, and self-replication [13-15], they are now regarded as seed cells for a wide range of applications in tissue engineering and biotherapy. HUC-MSCs have unique merits over bone marrow and adipose-derived MSCs in that they present no substantial ethical challenges, exhibit a low risk of viral transmission [16], have low immunogenicity, as well as being readily available and more primitive [17]. HUC-MSCs have received more attention in the treatment of cancer. HUC-MSCs inhibit tumor growth by secreting relevant cytokines on their own. Studies have shown that HUC-MSCs can induce apoptosis and promote benign progression in esophageal, ovarian, and leukemia cancer cells [18-20]. Furthermore, HUC-MSCs have stem cell characteristics, which means they can easily cross the blood-brain barrier and have tumor tropism [21]. As a result, it can be used as a therapy to treat GBM. Although HUC-MSCs have been reported to be anti-GBM [21], there is a lack of exploration of extracting the supernatants of HUC-MSCs at different times to resist GBM.

Signal transducer and activator of transcription (STAT) proteins belong to a family of cytoplasmic transcription factors that can bind to DNA [22]. The STAT family consists of seven structurally and functionally related proteins STAT1, STAT2, STAT3, STAT4, STAT5a, STAT5b, and STAT6 [23]. Of these,

STAT3 is involved in a variety of biological processes, such as angiogenesis, cell proliferation, survival, and differentiation [24, 25]. Upon tyrosine phosphorylation by receptor-associated tyrosine kinases, STAT3 translocates to the nucleus and activates the expression of downstream genes to regulate tumor cell growth, proliferation, differentiation, and metastasis [26]. Previous studies have shown that the translocation and activation of STAT3 are affected by some factors that may enhance STAT3 activity, such as IL-6, Janus kinase 2 (JAK2), LIF, and EGF [27-29]. In addition, Protein inhibitors of activated STAT3 (PIAS3) that bind to STAT3 have been identified [31]. The binding of PIAS3 to STAT3 is only observed in cells that cause STAT3 activation. The DNA binding activity of STAT3 is blocked by PIAS3, thereby inhibiting STAT3-mediated downstream gene activation [30]. PIAS3 is upregulated to inactivate STAT3, promoting apoptosis and autophagy in tumor cells. STAT3 plays a crucial role in multiple human cancers, especially in GBM, and it is in an over-activated state that is often associated with poor clinical prognosis [31]. p-STAT3 was reported to affect the occurrence, development, and even prognosis of GBM [32, 33]. However, whether HUC-MSCs supernatant mediates STAT3 inactivation in GBM cells remains unknown. We performed multiple experiments involving western blot, laser confocal, and Immunocytochemical Staining (ICC) to explore the mechanism of IL-6/JAK2/STAT3 signaling pathway regulation in GBM cells. And reported that C188-9 is a potent STAT3 inhibitor, which can target the phosphotyrosine (pY) peptide binding site in the STAT3 Src-homology (SH)2 domain [34, 35] to inhibit STAT3 activation. Based on this, novel therapeutic strategies targeting the IL-6/JAK2/STAT3 signaling pathway may open up new avenues for the regulation of long-term multilevel regulation of GBM cells.

Materials and Methods

Isolation, Culture, and Identification of HUC-MSCs

Umbilical cord tissues were obtained from healthy fetuses delivered by cesarean section at full term in the Obstetrics Department of Yan'an University Affiliated Hospital. With the approval of the Biomedical Ethics Committee of the Yan'an University School of Medicine, these umbilical cord tissues were obtained with the knowledge and permission of the mother and family. They were sent to Yan'an University Medical Experiment Center, where the umbilical cord tissue was isolated and cultured using the tissue block isolation method. The umbilical cord was repeatedly rinsed with saline to

remove blood stains and cut into 5 sections, one umbilical vein and two umbilical arteries were carefully removed, and then cut into 2-3 mm sized tissue pieces and for inoculation in 75 cm² culture flasks. The 75 cm² culture flask inoculated with umbilical cord tissue blocks was inverted and placed in a 37°C, 5% CO₂ cell culture incubator for 6 h, then 3-4 ml of HUC-MSCs complete medium (Procels Life Science Technology Co., Ltd.) was added. Cells could be seen crawling out from around the tissue block until about 7 days. The first passages could be made when the cells reached 80%-90% of the culture flask.

Collection of HUC-MSCs Supernatants and Preparation of Lyophilized Powder

When P3-P8 generation HUC-MSCs grew to 80%-90% fused state, culture flasks full of HUC-MSCs were rinsed with PBS, and trypsin was added to each flask and digested for 2-3 min, then digestion was terminated with H-DMEM containing 10% FBS. The terminated cell suspension was collected and centrifuged at 1000 rpm for 5 min, discarded the supernatants and HUC-MSCs were harvested. The HUC-MSCs were inoculated according to 7×10⁵ cells/75cm² cell culture flasks, and HUC-MSCs supernatants were collected in two approaches. In one approach, HUC-MSCs were incubated with 8-9 ml of H-DMEM containing 10% FBS for 24 h and replaced by 14 ml of H-DMEM without FBS for 24 h, 48 h, and 72 h respectively, and then HUC-MSCs supernatants were collected. After freezing and solidifying at -80°C, the frozen solidified supernatants were placed in a pre-cooled vacuum for evacuation, sublimated, and dried to prepare a lyophilized powder, weighed and dissolved in cell grade PBS and filtered through a 0.22 µm/ml filter. The filtered supernatants were collected in sterile centrifuge tubes and frozen at 4°C for short-term or -20°C for long-term storage. Alternatively, HUC-MSCs supernatants were collected using 8-9 ml of H-DMEM containing 10% FBS incubated for 24 h, 48 h, and 72 h replacement of 14 ml of H-DMEM without FBS for 24 h respectively, frozen solidified at -80°C, the frozen solidified supernatants were placed in a pre-cooled vacuum machine to evacuate, sublimated, and dried to prepare a lyophilized powder, weighed, dissolved in cells-grade PBS, filtered through a 0.22 µm/ml filter and the filtered supernatants were collected in sterile centrifuge tubes and stored frozen at 4°C for short-term storage or -20°C for long-term storage.

GBM cells Culture and Cells Treatments

Human glioma cells U251, human brain astrocytoma cells U87-MG, and Human glioblastoma cells LN-428 were purchased from Otwo Biotech

(Guangzhou, China). Rat glioma cells RG-2 cells were obtained from Ya Ji Biological (Shanghai, China). All cells were cultured in H-DMEM complete medium (GIBCO, Invitrogen) with a volume fraction of 10% fetal bovine serum (FBS, GIBCO, Invitrogen) and 1% penicillin-streptomycin (Solarbio, Beijing, China) at 37°C in a volume fraction of 5% CO₂. RG-2, U251, U87-MG, and LN-428 cells were conditioned with 9 mg/ml of HUC-MSCs supernatants for 48 h. A total of 3×10⁵ cells were mounted on culture dishes (Nunc A/S, Roskilde, Denmark) and cultured for 24 h before further experiments. Dozens of cells-bearing coverslips were concurrently prepared under the same experimental condition using the high throughput coverslip-preparation dishes (Jet Biofile Tech. Inc., Guangzhou, China, China invention patent No. ZL200610047607.8), which were collected during drug treatments, fixed with cold acetone, and used for hematoxylin, and eosin (H&E) staining, and terminal deoxynucleotidyl transferase dUTP nick end labeling (TUNEL, Transgen, China) apoptosis assay.

Cells Proliferation Assay

To determine the effect of GBM cells U251, U87-MG, LN-428, and RG-2 after incubation with HUC-MSCs supernatants or/and C188-9 (Alias: TTI-101, Sperkjade, China). U251, U87-MG, LN-428, and RG-2 were inoculated on a 96-well plate and incubated with HUC-MSCs supernatants for 24 h, 48 h, and 72 h. Cell proliferation was analyzed by the Cells Counting Kit-8 assay (CCK-8, DOJINDO, Japan). The supernatants of HUC-MSCs were treated on U251, U87-MG, LN-428, and RG-2 cells for 48 h. Afterward, it was collected, resuspended with pre-cooled PBS, and then resuspended with 70% cold ethanol at -20°C overnight. The following day, cells were rinsed with pre-chilled PBS and stained using RNase and propidium iodide (PI) according to the manufacturer's instructions. Subsequently, the cell cycle was analyzed by NovoExpress (Agilent Technologies, USA).

Annexin V/PI Staining Assay

The Annexin V-FITC Apoptosis Detection Kit (Nanjing Key Gen Biotech Co., Nanjing, China) was used for the quantification of apoptosis. 6×10⁵ cells per dish were seeded into 60 mm culture plates and collected after 48 h of HUC-MSCs supernatants treatment. Externalized phosphatidylserine was labeled with Annexin V-FITC conjugated for 15 min on ice. Propidium iodide (PI, 1 µg/mL) was added 10 min prior to FACS analysis. Active (annexin-/PI-), early (annexin+/PI-) and late apoptotic (annexin+/PI+) and necrotic cells (annexin-/PI+) were assigned. The labeled cells were identified by flow cytometry.

Migration and Invasion Assays

Transwell chambers were assayed for cell migration invasion ability by applying 50 μ l of Matrigel gel (1: 4 dilution) to the transwell chambers to be checked and incubated at 37°C for 30 min to form a gel. Approximately 3×10^4 cells were inoculated onto the Matrigel gel-coated chambers and kept in an FBS-free cell culture medium with a concentration of 0 mg/ml or 9 mg/ml of HUC-MSCs supernatants or/and C188-9. H-DMEM containing 10% FBS was added to the lower chamber. The cells were incubated at 37°C and 5% CO₂ for 24 h, fixed with 4% paraformaldehyde for 30 min, and stained with 0.1% crystalline violet for 20 min. Five fields of view were randomly selected for filming. Assessment of the migratory capacity of GBM cells was performed in the same steps as for the invasion assay, but without Matrigel.

Immunocytochemical Staining/ICC

RG-2, U251, U87-MG, and LN-428 cells were conditioned with 9 mg/ml HUC-MSCs supernatants for 48 h. A total of 3×10^5 cells were plated into culture dishes (Nunc A/S, Roskilde, Denmark) and cultured for 24 h before further experiments. Cells were collected after 48 h of drug treatment and fixed in 4% paraformaldehyde. Coverslips containing cells from each experimental group were subjected to ICC according to the SABC Immunohistochemical Staining Kit (Boster, California, USA). Briefly, Coverslips were washed with PBS (pH 7.4), incubated in 3% H₂O₂ for 10 min, and then incubated overnight at 4°C with the appropriate dilution of the first antibodies. The antibodies used were: IL-6 Polyclonal antibody (proteintech, 1: 1000), Rabbit Anti-JAK2 antibody (Bioss, 1: 500), STAT3 monoclonal antibody (ABclonal, China, 1: 200), phosphatidyl STAT3-Y705 rabbit pAb (ABclonal, China, 1: 200), PIAS3 (ABclonal, China, 1: 100), Survivin (ABclonal, China, 1: 100), VEGFA (ABclonal, China, 1: 100), Bcl-2 (proteintech, 1: 500), MCL-1 monoclonal antibody (ABclonal, China, 1: 100), c-Myc monoclonal antibody (Proteintech, 1: 100), Caspase-3 monoclonal antibody (Proteintech, 1: 500), Mouse Anti-Active Caspase 3 monoclonal antibody (Bioss, 1: 500) Caspase 8 monoclonal antibody (Proteintech, 1: 500), MMP-2 monoclonal antibody (Proteintech, 1: 500), MMP-9 monoclonal antibody (Proteintech, 1: 500). Treatment with biotin-labeled goat anti-rabbit IgG for 20 min, followed by treatment with streptavidin-peroxidase complex for 20 min. Reactions were carried out using DAB chromogenic kit (DAB, Boster, California, USA). The staining results were evaluated by two independent researchers, depending on the intensity of the marker. If no immunolabelling was observed in

the target cells, it was negative (-). Weakly positive (+) if the marker is faint. Moderately positive (++) Strongly positive (>++) if the marker is strong or significantly stronger than (++)

Triple Immunofluorescent Labeling/IF

For triple immunofluorescence staining (IF), the coverslips with cells were rinsed by using phosphate-buffered saline (PBS, pH 7.4), fixed in 4% paraformaldehyde for 20 min, incubated in 0.1% Triton-X100 for 5 min, and closed with 3% BSA for 2 h. Primary antibodies LC3 II/I (ABclonal, China, 1: 200) and Beclin-1 (Proteintech, Chicago, IL, USA, 1: 500) were mixed, and the coverslips were hatched overnight at 4°C overnight, coverslips were incubated with mouse anti-CoraLite488-conjugated goat anti-mouse IgG (H+L) and rabbit anti-Cy3-conjugated Affinipure goat anti-rabbit IgG (H+L) for 2 h. DAPI (Boster, California, USA) was incubated for 10 min to localize cell nuclei, mounted with an anti-fluorescence quenching sealing liquid (Solarbio, Beijing, China), observed and imaged in Laser Confocal Microscope (LSM800, ZEISS, Oberkochen, Germany).

Western Blot Analysis

For Western Blot analyses, total cellular proteins were prepared from cells cultured under 9 mg/ml HUC-MSCs supernatants conditions. 50 μ g/well or 30 μ g/well of the sample proteins were separated by electrophoresis in 10% sodium dodecylsulfate-polyacrylamide gel electrophoresis (SDS-PAGE) and transferred to Millex-Millipore® 0.45 μ m polypropylene difluoride membrane (Millipore®, MA, USA). The membranes were blocked with 10% skim milk in TBS-T (10 mM Tris-Cl, pH 8.0, 150 mM NaCl, and 0.5% Tween 20) at 37°C for 2 h, followed by incubation with the appropriate concentration of primary antibody overnight at 4°C. The antibodies used were: IL-6 Polyclonal antibody (proteintech, 1: 1000), Rabbit Anti-JAK2 antibody (Bioss, 1:500), STAT3 monoclonal antibody (ABclonal, China, 1: 1000), phosphatidyl STAT3-Y705 rabbit pAb (p-stat3, ABclonal, China, 1: 1000), PIAS3 (ABclonal, China, 1: 1000), Survivin (ABclonal, China, 1: 1000), VEGFA (ABclonal, China, 1: 1000), Bcl-2 (proteintech, 1: 1000), MCL-1 monoclonal antibody (ABclonal, China, 1: 1000), c-Myc monoclonal antibody (proteintech, 1: 1000), LC3 II/ I (ABclonal, China, 1: 2000) and Beclin-1 (Proteintech, Chicago, IL, USA, 1: 2000), Caspase 3 monoclonal antibody (proteintech, 1: 1000), Mouse Anti-Active Caspase 3 monoclonal antibody (Bioss, 1:1000), Caspase 8 monoclonal antibody (Proteintech, 1: 1000), MMP-2 monoclonal antibody (Proteintech, 1: 1000), MMP-9 monoclonal antibody (Proteintech, 1: 1000), Cyclin A2 (Proteintech, 1: 1000),

CDK2 (Proteintech, 1: 1000), Cyclin D1 (Proteintech, 1: 1000) and CDK4 (Proteintech, 1: 1000). Subsequently, the membranes were incubated with HRP-conjugated anti-mouse or anti-rabbit IgG (Proteintech, Chicago, IL, USA) for 1.5 h. The bound antibodies were detected by enhanced chemiluminescence. Bound antibodies were detected using an enhanced chemiluminescence system (Syngene, India). The same experimental procedure was used for replating one by one with other antibodies until all parameters were checked.

Statistical Analysis

Statistical analysis was performed by using Graphpad Prism 9.0 software (Graph-pad Software Inc., San Diego, CA). Two-way repeated measures ANOVA and two-tailed Student's t-test were used. $P < 0.05$ was considered statistically significant. The bar graphs present the mean \pm standard deviation (SD) of the experimental data.

Table 1: Grouping of glioma cells treated with HUC-MSC culture supernatant.

Cells Lines	Group	HUC-MSCs Supernatant Extract Concentration (mg/ml)	Incubation Time (hours)
RG-2	0-24	0	24
			48
			72
	1-24	1	24
			48
			72
	3-24	3	24
			48
			72
	6-24	6	24
			48
			72
	9-24	9	24
			48
			72
U251	0-24	0	24
			48
			72
	1-24	1	24
			48
			72
	3-24	3	24
			48
			72
6-24	6	24	
		48	
		72	
9-24	9	24	
		48	
		72	
U87-MG	0-24	0	24
			48
			72
	1-24	1	24
			48
			72
	3-24	3	24
			48
			72
6-24	6	24	
		48	
		72	

Cells Lines	Group	HUC-MSCs Supernatant Extract Concentration (mg/ml)	Incubation Time (hours)	
LN-428	6-72	9	72	
			24	
			48	
	9-72	0	0	24
				48
				72
	1-24	1	1	24
				48
				72
	3-24	3	3	24
				48
				72
	6-24	6	6	24
				48
				72
9-24	9	9	24	
			48	
			72	

Results

HUC-MSCs Supernatants Collected by Different Methods Suppressed the Growth of GBM Cell Lines

We used two approaches to collect HUC-MSCs supernatants. One approach was to incubate HUC-MSCs with 8-9 ml of H-DMEM containing 10% FBS for 24 h and then with 14 ml of H-DMEM without FBS for 24 h, 48 h, and 72 h, respectively. Alternatively, HUC-MSCs supernatants were collected using 8-9 ml of H-DMEM containing 10% FBS incubated for 24 h, 48 h, and 72 h replacement of 14 ml of H-DMEM without FBS for 24 h, respectively. Subsequently, we assessed the effect of HUC-MSCs supernatants on the cell viability of U251, U87-MG, LN-428, and RG-2. We used two methods to collect HUC-MSCs supernatants that were divided into five different concentrations for the treatment of U251, U87-MG, LN-428, and RG-2 respectively for CCK-8 assay. The concentration of HUC-MSCs supernatants extracts and the treatment grouping of GBM cells were shown in Table 1. From the CCK-8 results, we observed that HUC-MSCs supernatants were maintained for 24 h, 48 h, and 72 h with varying sensitivity levels of U251, U87-MG, LN-428, and RG-2 to HUC-MSCs supernatants. U251, U87-MG, LN-428, and RG-2 showed concentration-dependent but not time-dependent inhibition. After the treatment of HUC-MSCs supernatants, we found that RG-2 cells were the most sensitive, followed by LN-428 and U87-MG, and U251 was the least sensitive (Fig. 1A and 1B). In particular, 9 mg/ml HUC-MSCs supernatants collected after 48 h incubation with H-DMEM containing 10% FBS replaced by H-DMEM without FBS for 24 h showed significant inhibition of the growth of U251, U87-MG, LN-428, and RG-2. For instance, after 48 h of treatment with 9 mg/ml

HUC-MSCs supernatants, the cells viability of RG-2 was $19.96 \pm 6.11\%$ ($P < 0.001$), that of LN-428 was $63.93 \pm 2.80\%$ ($P < 0.001$). However, cell viability was $85.19 \pm 2.90\%$ ($P < 0.01$) and $78.55 \pm 8.078\%$ ($P < 0.01$) for U251 and U87-MG respectively. Overall, HUC-MSCs supernatants could selectively target GBM cells for toxic effects. Combining the results of the CCK-8 assay from both methods, we used H-DMEM containing 10% FBS for 48 h, then replaced H-DMEM without FBS to continue incubation for 24 h before collecting 9 mg/ml HUC-MSCs supernatants as the effective concentration for subsequent experiments (Fig. 1C).

To further determine the tumor-suppressive effect of U251, U87-MG, LN-428, and RG-2 by HUC-MSCs supernatants, we performed H&E morphological staining. The results showed that all GBM cells in normal culture were densely grown and morphologically plump, however, the morphological changes of the four cell types were different after treatment with 9 mg/ml of HUC-MSCs supernatants. RG-2 and LN-428 cells were partially crinkled and rounded, U87-MG cells were flattened and elongated, and U251 cells did not change significantly in morphology. At the same time, the number of cells in these four cell lines was reduced (Fig. 1D). In

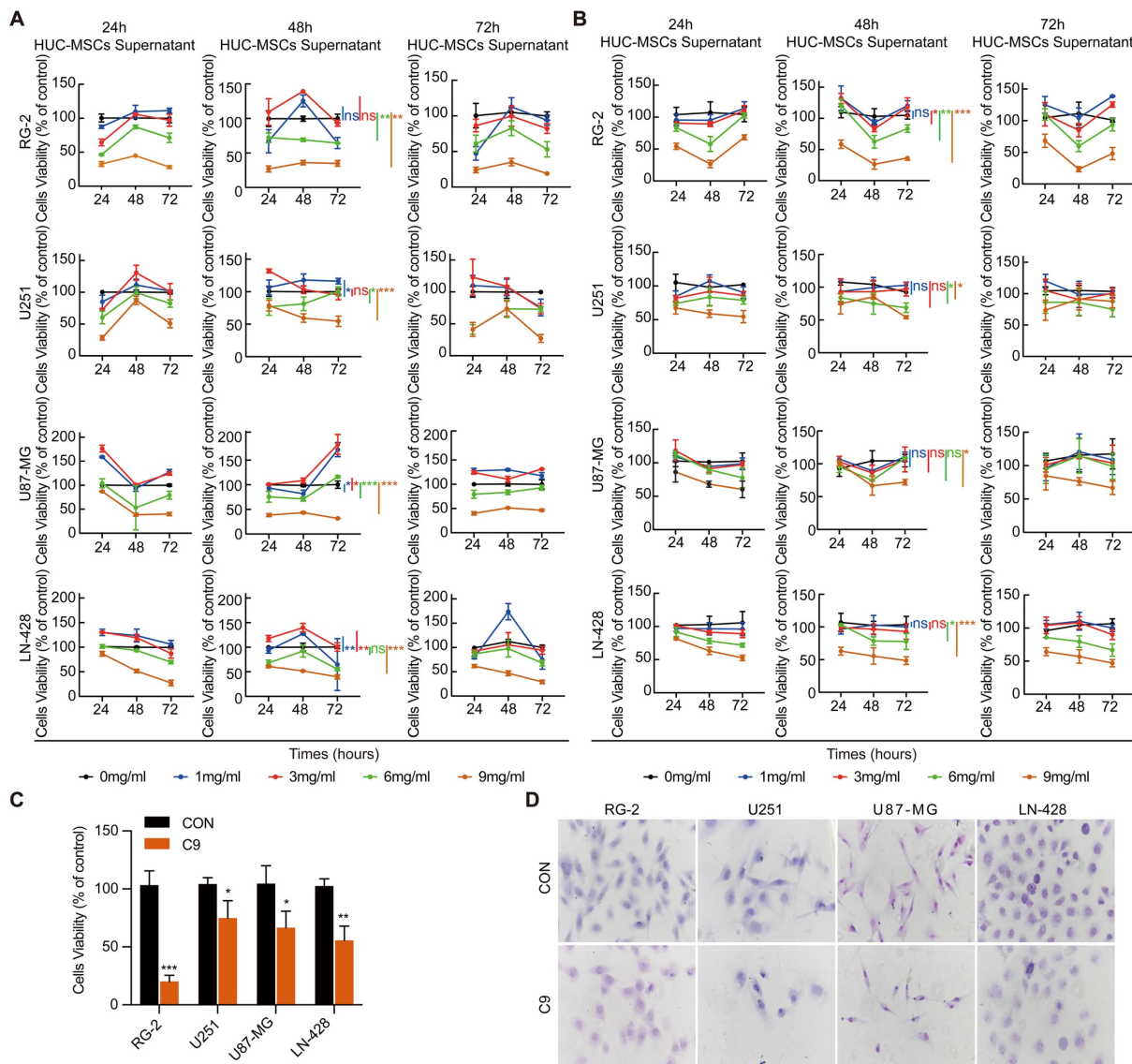


Figure 1. Growth inhibition of GBM cells by HUC-MSCs supernatant. **(A), (B)** and **(C)** CCK-8 assays: **(A)** HUC-MSCs were incubated with H-DMEM containing 10% FBS for 24 h and replaced by H-DMEM without FBS for 24 h, 48 h, and 72 h respectively, and then HUC-MSCs supernatants were collected. U251, U87-MG, LN-428, and RG-2 cells were treated with the collected HUC-MSCs supernatants for 24 h, 48 h, and 72 h, and then analyzed by the CCK-8 assay. **(B)** HUC-MSCs were incubated with H-DMEM containing 10% FBS for 24 h, 48 h, and 72 h, replaced by H-DMEM without FBS for 24 h. The HUC-MSCs supernatants were collected. U251, U87-MG, LN-428, and RG-2 cells were treated with the collected HUC-MSCs supernatants for 24 h, 48 h, and 72 h, respectively, and analyzed by the CCK-8 assay. **(C)** HUC-MSCs were incubated with H-DMEM containing 10% FBS for 48 h, replaced by H-DMEM without FBS, and continued for 24 h, then the collected supernatant of HUC-MSCs at 9 mg/ml was used as the effective concentration. **(D)** H&E morphological staining (inverted phase contrast microscope, $\times 40$) was detected in GBM cells and treated for 48 h in the absence (CON) or presence (C9) of 9 mg/ml HUC-MSCs supernatants. HUC-MSCs supernatants, Human Umbilical Cord Mesenchymal Stem Cell Supernatants. $**P < 0.01$, and $***P < 0.001$ vs CON group; the error bars, the mean \pm standard deviation.

summary, HUC-MSCs supernatants inhibited the growth of GBM cells and influenced cell morphology.

HUC-MSCs Supernatants Inducing GBM Cells to Arrest in G0/G1 or S Phase

Cell cycle alterations are often influenced by cell proliferation. RG-2, U251, U87-MG, and LN-428 cell proliferation was inhibited by HUC-MSCs supernatants (Fig. 1C and D). To test whether HUC-MSCs supernatants affected the GBM cell cycle, we analyzed cell cycle changes by flow cytometry. The results showed that RG-2, U251, and U87-MG cells were stalled in the S phase by HUC-MSCs supernatants (Fig. 2A). In contrast, LN-428 cells were induced to stagnate in G0/G1 phase (Fig. 2A). We examined the expression levels of proteins associated with the corresponding cell cycle, such as Cyclin A2, CDK2, Cyclin D1, and CDK4, to further validate the effect of HUC-MSCs supernatants on the GBM cell cycle. Western Blot results suggested that the expressions of Cyclin A2, and CDK2 were reduced in RG-2, U251 and U87-MG treated with 9 mg/ml HUC-MSCs supernatants for 48 h. That is, Cyclin A2 expressions were reduced by 53%, 38%, and 70% in RG-2, U251, and U87-MG cells, and CDK2 expressions by 30%, 36%, and 62% respectively (Fig. 2B). The expressions of Cyclin D1 and CDK4 were reduced by 58%, and 35% in LN-428 cells treated with 9 mg/ml HUC-MSCs supernatants for 48 h (Fig. 2B). In summary, RG-2, U251 and U87-MG cells by

HUC-MSCs supernatants were induced to block in S phase, whereas LN-428 cells were blocked in G0/G1 phase.

HUC-MSCs Have the Ability to Tumor Tropism

The main challenge of anticancer drugs is poor tumor targeting [36]. MSCs possess an inherent potential for tumor tropism and can serve as an ideal candidate [36]. To test whether HUC-MSCs have tumor tropism *in-vitro*, we determined by the transwell assay that HUC-MSCs have tumor-specific tropism in RG-2, U251, U87-MG, and LN-428 cells (Fig. 2C), which provides a strong *in-vitro* experimental basis for targeted therapy of GBM.

HUC-MSCs Supernatants Caused GBM Cells Apoptosis

To detect the apoptosis of GBM cells were affected by HUC-MSCs supernatants, GBM cells U251, U87-MG, LN-428, and RG-2 were treated with HUC-MSCs supernatants for 48 h and the changes in apoptosis of GBM cells were detected by TUNEL assay. TUNEL assay is used to detect DNA breaks formed during the final phase of apoptosis when DNA fragmentation takes place. It is important to validate the induction of cell apoptosis by using DNA-fragmentation assays. From our results, we could find that the cells in the experimental group frequently underwent apoptosis compared to the

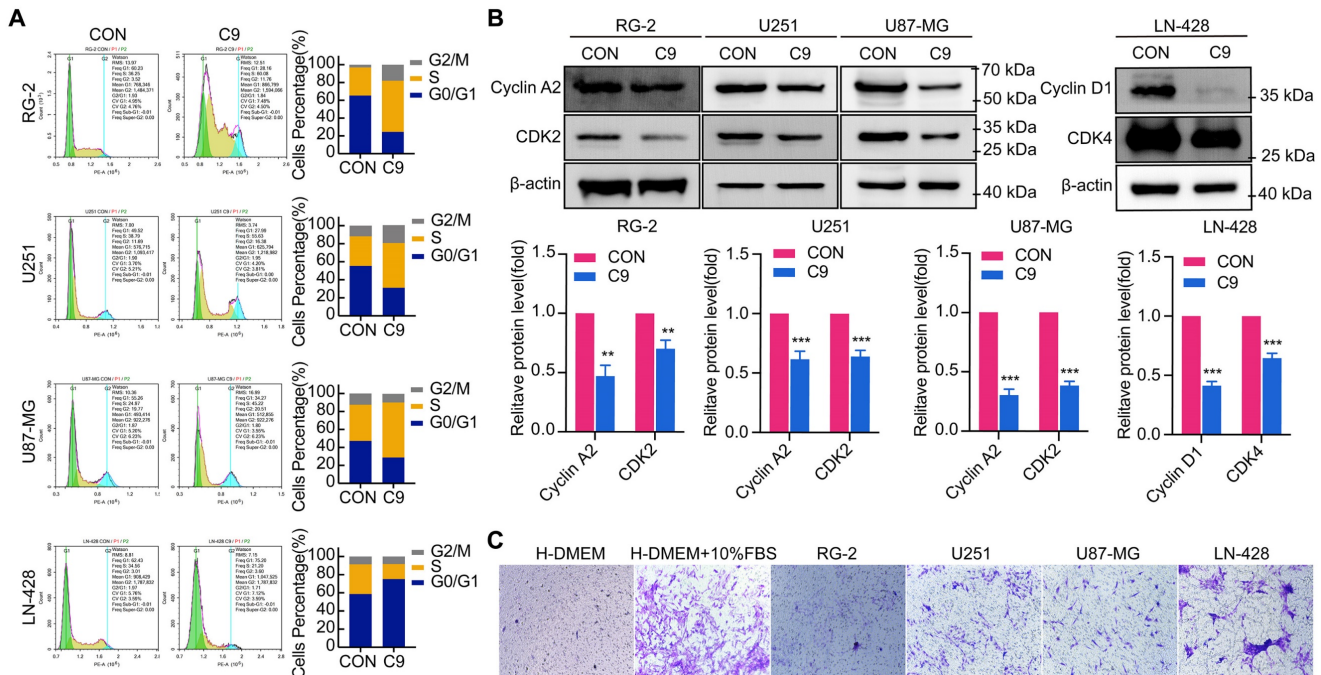


Figure 2. Cell cycle of U251, U87-MG, LN-428, and RG-2 cells was altered after treatment with 9 mg/ml HUC-MSCs supernatants for 48 h, and HUC-MSCs had tumor tropism. (A) Cell cycle distribution was detected with PI staining. (B) Western Blot. β -actin was used as a qualitative and quantitative control. (C) Transwell experiments confirmed *in vitro* that HUC-MSCs could migrate to GBM cells. CON, 0 mg/ml HUC-MSCs supernatant; C9, 9 mg/ml HUC-MSCs supernatants; * $P < 0.05$, ** $P < 0.01$ and *** $P < 0.001$ vs CON group; the error bars, the mean \pm standard deviation.

control group. The apoptosis of RG-2 was the most pronounced, followed by U251 and U87-MG (Fig. 3A). LN-428 apoptosis was less pronounced than that of RG-2, U251, and U87-MG (Fig. 3A). To further verify that GBM cell apoptosis was affected by HUC-MSCs supernatants, we examined the treatment of GBM cells with HUC-MSCs supernatants for 48 h by flow cytometry. The results suggested that after GBM cells were treated with HUC-MSCs supernatants, the percentages of early, late and total apoptotic cells in the RG-2 cells were 24.60% (4.75% in control), 6.76% (1.22% in control) and 31.36% (5.97% in control), respectively. The percentages of early, late, and total apoptotic cells in U251 cells were 14.2% (4.53% in control), 2.44% (1.15% in control), and 16.64% (5.68% in control), respectively. The percentages of early, late, and total apoptotic cells in U87-MG cells were 17.5% (4.93% in control), 2.53% (1.09% in control), and 20.03% (6.02% in control), respectively. The percentages of early, late, and total apoptotic cells in LN-428 cells were 5.20% (1.88% in control), 3.35% (1.62% in control), and 8.55% (3.50% in control) respectively (Fig. 3B). From the above results, it can be seen that HUC-MSCs supernatants promoted apoptosis of GBM cells compared to the control, especially RG-2 ($P < 0.001$) and U87-MG ($P < 0.001$). U251 ($P < 0.01$) was slightly weaker than that of RG-2 and U87-MG, and apoptosis in these three cells occurred at an early stage. However, the apoptotic effect of HUC-MSCs supernatants on LN-428 ($P < 0.05$) was significantly poorer (Fig. 3B and E).

We also examined the expression of proteins associated with GBM apoptosis, such as Bcl-2, Caspase 3, Cleaved-Caspase 3, and Caspase 8. Western Blot results suggested that the expression levels of Bcl-2, Caspase 3, Cleaved-Caspase 3, and Caspase 8 were affected by HUC-MSCs supernatants. In RG-2 cells, compared to the control group, the expression levels of the anti-apoptotic protein Bcl-2 were weakened (65% reduction), and the expression levels of the pro-apoptotic proteins Caspase 3 (42% increase), Cleaved-Caspase 3 (39% increase) and Caspase 8 (62% increase) were increased in the treatment group. In U251, U87-MG, and LN-428, the expression levels of the anti-apoptotic protein Bcl-2 were attenuated (35%, 42%, and 42% reduction). The expression levels of pro-apoptotic proteins Caspase 3 (31%, 39%, and 77% increase), Cleaved-Caspase 3 (61%, 55%, 57% increase), and Caspase 8 (31%, 36%, and 62% increase) were increased in the treated group compared to the control group (Fig. 3C). The results of ICC further supported the above inference (Fig. 3D). These data suggested that GBM cell apoptosis was promoted by HUC-MSCs supernatants.

HUC-MSCs Supernatants Inhibited GBM Cells Migration and Invasion

Transwell experiments were used to determine whether HUC-MSCs supernatants affect the migration and invasion of GBM cells, we discovered that HUC-MSC supernatants blocked the migration and invasion abilities of GBM cells. The results showed that the migratory ability of GBM cells was significantly affected by HUC-MSCs supernatants in RG-2, U251, and U87-MG cells compared to the control group, especially in RG-2 cells. However, HUC-MSCs supernatants had no effect on LN-428 migratory ability, and quantification revealed no statistical difference $P > 0.05$ (Fig. 4A and C). The Transwell invasion assay results for RG-2, U251 and U87-MG showed the same results as the migration assay. In contrast, the effect of HUC-MSCs supernatants on the invasion ability of LN-428 was existed but weak (Fig. 4B and D). To further confirm that HUC-MSCs supernatants affected GBM cell migration and invasion, we examined the expression of proteins associated with GBM cell migration and invasion, such as MMP-2, MMP-9, and VEGFA. MMP-2, MMP-9, and VEGFA expression were reduced in RG-2, U251, U87-MG, and LN-428 after 48 h of treatment with 9 mg/ml HUC-MSCs supernatants, according to Western blot results. That is, the expressions of MMP-2 (82%), MMP-9 (52%), and VEGFA (44%) were most significantly diminished in U87-MG cells. The migratory and invasive abilities of RG-2 and U251 were weaker than those of U87-MG, with MMP-2 expressions reduced by 47% and 37%, respectively, in RG-2 and U251 cells, and MMP-9 expressions by 40% and 20%, respectively. VEGFA expression was reduced by 30% and 40% in RG-2 and U251 cells, respectively. The expressions of MMP-2 (30%), MMP-9 (13%), and VEGFA (37%) were the worst in LN-428 cells (Fig. 4E and Fig. 6B). The results of ICC further supported the above inference (Fig. 4F and Fig. 6A). In summary, the migratory and invasive ability of GBM cells was inhibited by HUC-MSCs supernatants.

HUC-MSCs Supernatants Inhibited GBM Cell Growth through Down-regulation of IL-6/JAK2/STAT3 Expression

The IL-6/JAK2/STAT3 signaling pathway plays a critical role in the progression of glioma [27, 37]. As a result, we investigated whether HUC-MSCs supernatants could influence the function of the IL-6/JAK2/STAT3 signaling pathway in GBM cells. We extracted total protein from HUC-MSCs supernatant-sensitive RG-2, U87-MG, and LN-428 cells without and with 9 mg/ml HUC-MSCs supernatants treatment for ICC and Western Blot

analysis. Consistent with these clinical findings [27], our findings confirmed an increase in IL-6 and JAK2

expression in GBM cells RG-2, U251, U87-MG, and LN-428.

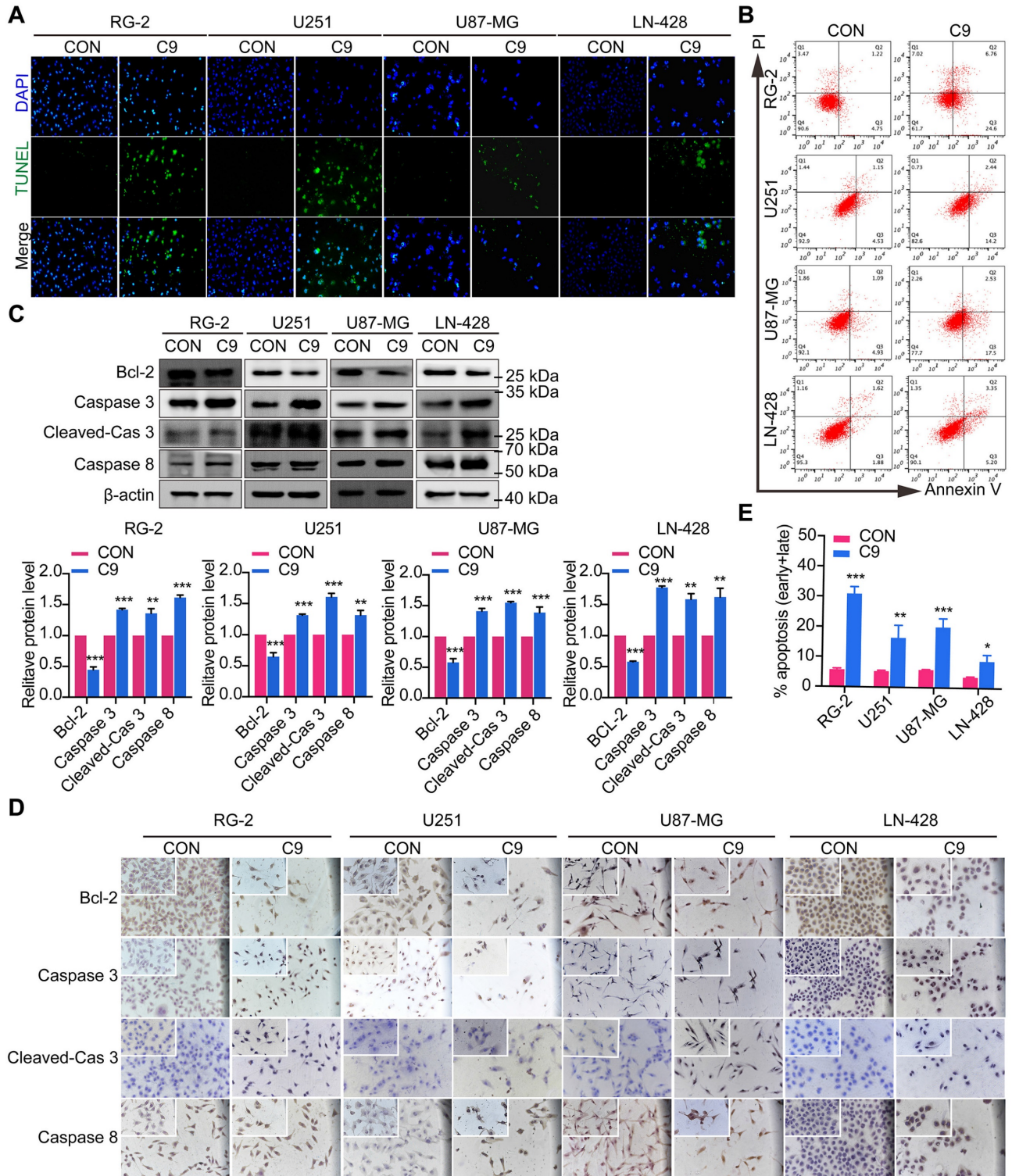


Figure 3. Apoptosis of U251, U87-MG, LN-428, and RG-2 cells after 48 h treatment with HUC-MSCs supernatants. **(A)** The images of the TUNEL apoptosis assay ($\times 20$). **(B)** Flow cytometry analysis of Annexin V and PI in four kinds of GBM cell lines for apoptosis. **(C)** and **(D)** Expression of apoptosis-related proteins Bcl-2, Caspase 3, and Caspase 8. **(C)** Western Blot. β -actin was used as a qualitative and quantitative control. **(D)** ICC ($\times 20$ and $\times 40$). **(E)** Apoptosis of the four GBM cell lines tested by flow cytometry was statistically analyzed. CON, 0 mg/ml HUC-MSCs supernatant; C9, 9 mg/ml HUC-MSCs supernatants; TUNEL, Terminal Deoxynucleotidyl Transferase dUTP Nick End Labeling; ICC, Immunocytochemistry. * $P < 0.05$, ** $P < 0.01$ and *** $P < 0.001$ vs CON group; the error bars, the mean \pm standard deviation.

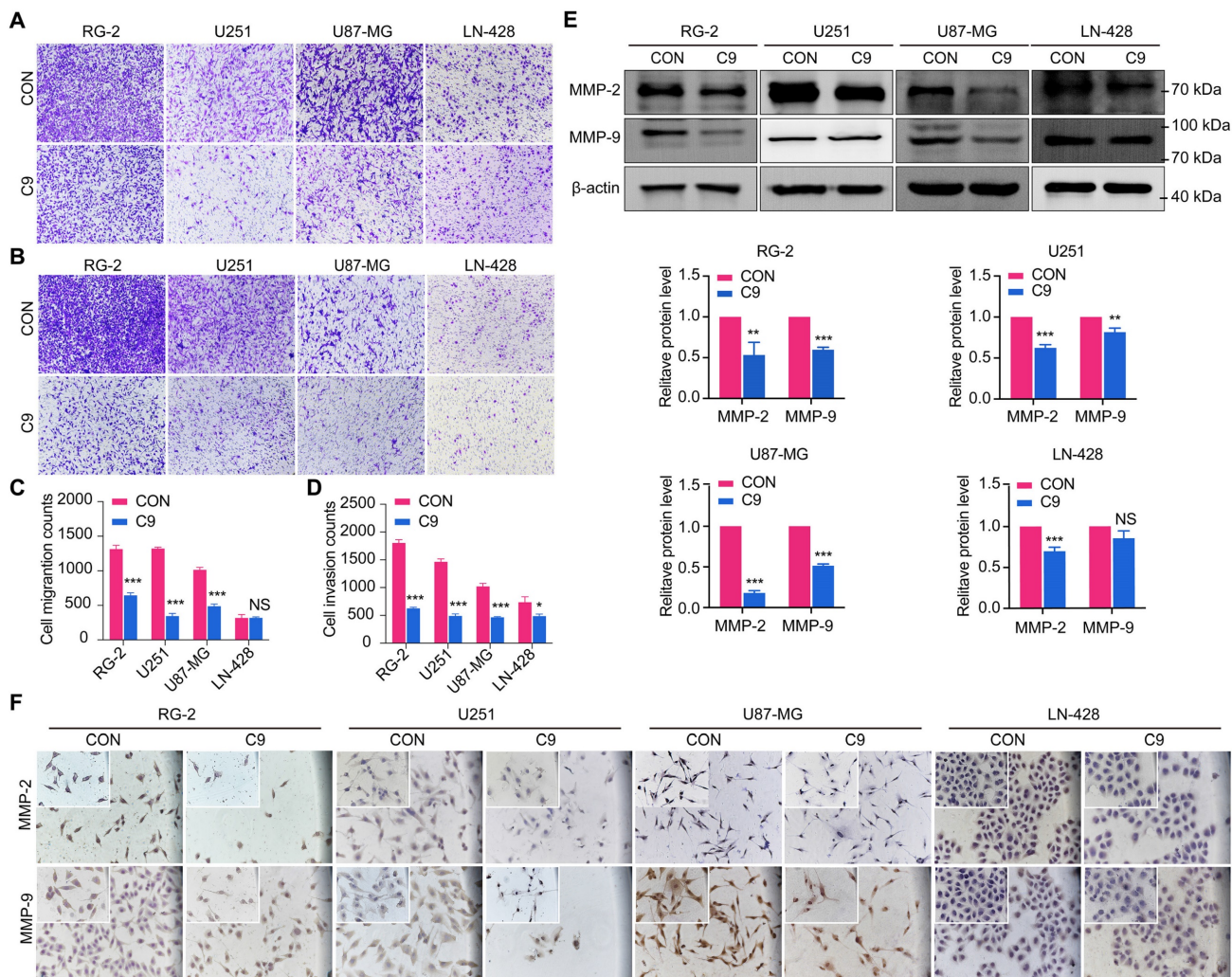


Figure 4. After 48 h treatment with 9 mg/ml HUC-MSCs supernatants, the migration and invasion ability of U251, U87-MG, LN-428, and RG-2 cells were inhibited. **(A)** Transwell Migration assay. **(B)** Transwell Invasion assay. **(C)** Four GBM cell lines were statistically analyzed for migration. **(D)** Four GBM cell lines were statistically analyzed for invasion. **(E)** and **(F)** Changes in the expression of migration-associated proteins MMP-2 and MMP-9 in GBM cells: **(E)** Western Blot. β -actin was used as a qualitative and quantitative control. **(F)** ICC. CON, 0 mg/ml HUC-MSCs supernatants; C9, 9 mg/ml HUC-MSCs supernatants; ICC, Immunocytochemistry. NS, no statistical significance ($P > 0.05$); * with statistical significance (* $P < 0.05$, ** $P < 0.01$, *** $P < 0.001$ vs CON group). The error bars, the mean \pm standard deviation.

However, the expression levels of IL-6 and JAK2 decreased after HUC-MSCs supernatants treatment for 48 h (Fig. 5A and B). From Western Blot results, we showed that U87-MG cells were treated with 9 mg/ml HUC-MSCs supernatants for 48 h, IL-6 expression was reduced by 54% compared to the control, and its expression was also decreased by different levels in RG-2 (50%), U251 (42%) and LN-428 (52%) cells, respectively. JAK2 expression was reduced in U87-MG (54%), RG-2 (52%), U251 (53%), and LN-428 (48%) cells (Fig. 5A and B). The results of ICC showed that STAT3 was expressed in all four normal cultured GBM cell lines with significant nuclear translocation, but after treatment with 9 mg/ml HUC-MSCs supernatants, the expression of STAT3 was down-regulated in the four GBM cell lines and nuclear translocation was also reduced (Fig. 5A). The results of Western Blot showed that after GBM cells were treated with 9 mg/ml HUC-MSCs supernatants

for 48 h, compared with the control group, the ratio of p-STAT3/STAT3 in RG-2, U251, and U87-MG cells was reduced by 33%, 35%, and 48%, respectively. This indicated that activated STAT3 was reduced in RG-2, U251, and U87-MG cells, especially in U87-MG cells. However, the expression level of p-STAT3 was higher than that of STAT3 in LN-428, which indicated that LN-428 was least inhibited by HUC-MSCs supernatant. Activated STAT3 is expressed at the p-STAT3 level. PIAS3 was lowly expressed in normally treated cells [30], whereas the expression of PIAS3 was elevated by 52% after 9 mg/ml HUC-MSCs supernatant treatment for 48 h. Phosphorylation of STAT3 was also inhibited in U251 (67%) and RG-2 (55%), and LN-428 (41%) cells after 48 h treatment with 9 mg/ml HUC-MSCs supernatants compared to the control, while PIAS3 was persistently highly expressed in U251 (79%) and RG-2 (64%) and LN-428 (51%) (Fig 5B). In conclusion,

the growth inhibition of GBM cells may be mediated by the STAT3 signaling pathway.

Growth Factor Reduction of STAT3 Signaling Pathway was Restrained by HUC-MSCs Supernatants

STAT3 downstream genes (MCL-1, Bcl-2, Survivin, VEGFA, and c-Myc) play an active role in cell proliferation and maintenance in gliomas [38, 39]. Therefore, we analyzed their expression status in four GBM cell lines with or without 9 mg/ml HUC-MSCs supernatants treatment. Western Blot and ICC results showed that MCL-1 levels decreased by 79% in HUC-MSCs supernatants-treated U87-MG cells after 48 h compared to the corresponding controls. HUC-MSCs supernatants-treated MCL-1 decreased by 45% in U251 cells, 45% in RG-2 cells, and 53% in LN-428 cells (Fig. 6A and B). In addition, the results showed that Survivin, VEGFA, and c-Myc levels were lower in U251, RG-2, LN-428, and U87-MG cells than in normal glioma cells. In particular, in U87-MG cells, Survivin, VEGFA, and c-Myc levels were 62%, 44%, and 39%, which were lower than those in normal

glioma cells (Fig. 6A and B). In conclusion, the above data suggested that the STAT3 signaling pathway is negatively regulated by HUC-MSCs supernatants, thus enabling improved GBM cells' therapeutic efficacy.

HUC-MSCs Supernatants Promoted Autophagy Downstream of STAT3 by Inhibiting the Signaling Pathway of STAT3

Whether HUC-MSCs supernatants effects autophagy in GBM cells through the STAT3 signaling pathway. We examined the proteins of RG-2, U251, U87-MG, and LN-428 cells after 48 h treatment with HUC-MSCs supernatants by IF assay. The autophagy-related proteins LC3 II/I and Beclin-1 were found to accumulate in RG-2, U251, U87-MG, and LN-428 cells (Fig. 6C). The results of the Western Blot analysis were consistent with the IF results. After treatment with 9 mg/ml HUC-MSCs for 48 h, the results suggested that the expressions of LC3 II/I, Beclin-1 were most significantly elevated in U87-MG cells by 80% and 55%. LC3 II/I, Beclin-1 was slightly less expressed in U251 and LN-428 cells. At the same

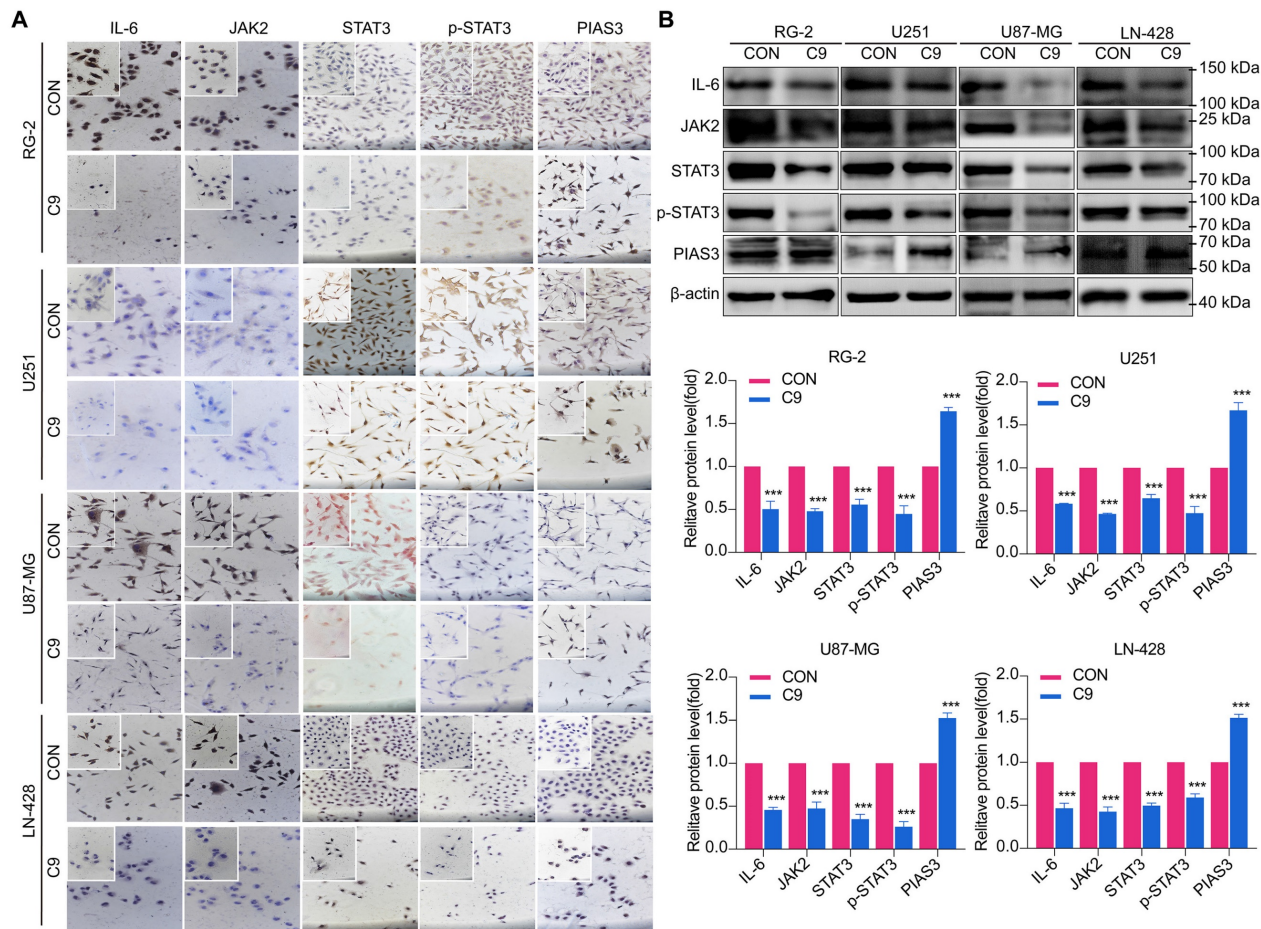


Figure 5. Changes in STAT3 signaling pathway in U251, U87-MG, LN-428, and RG-2 cells after 48 h treatment without (CON) or with (C9) HUC-MSCs supernatants. **(A)** ICC examination ($\times 20$ and $\times 40$), and **(B)** Western Blot analyses of IL-6, JAK2, STAT3, p-STAT3, and PIAS3. β -actin was used as a qualitative and quantitative control. CON, 0 mg/ml HUC-MSCs supernatants; C9, 9 mg/ml HUC-MSCs supernatants. * $P < 0.05$, ** $P < 0.01$ and *** $P < 0.001$ vs CON group; the error bars, the mean \pm standard deviation.

time, expression levels were lowest in LN-428 cells at 35% and 32% (Fig. 6D). Taken together, HUC-MSCs

supernatants can promote autophagy in GBM cells by negatively regulating the STAT3 signaling pathway.

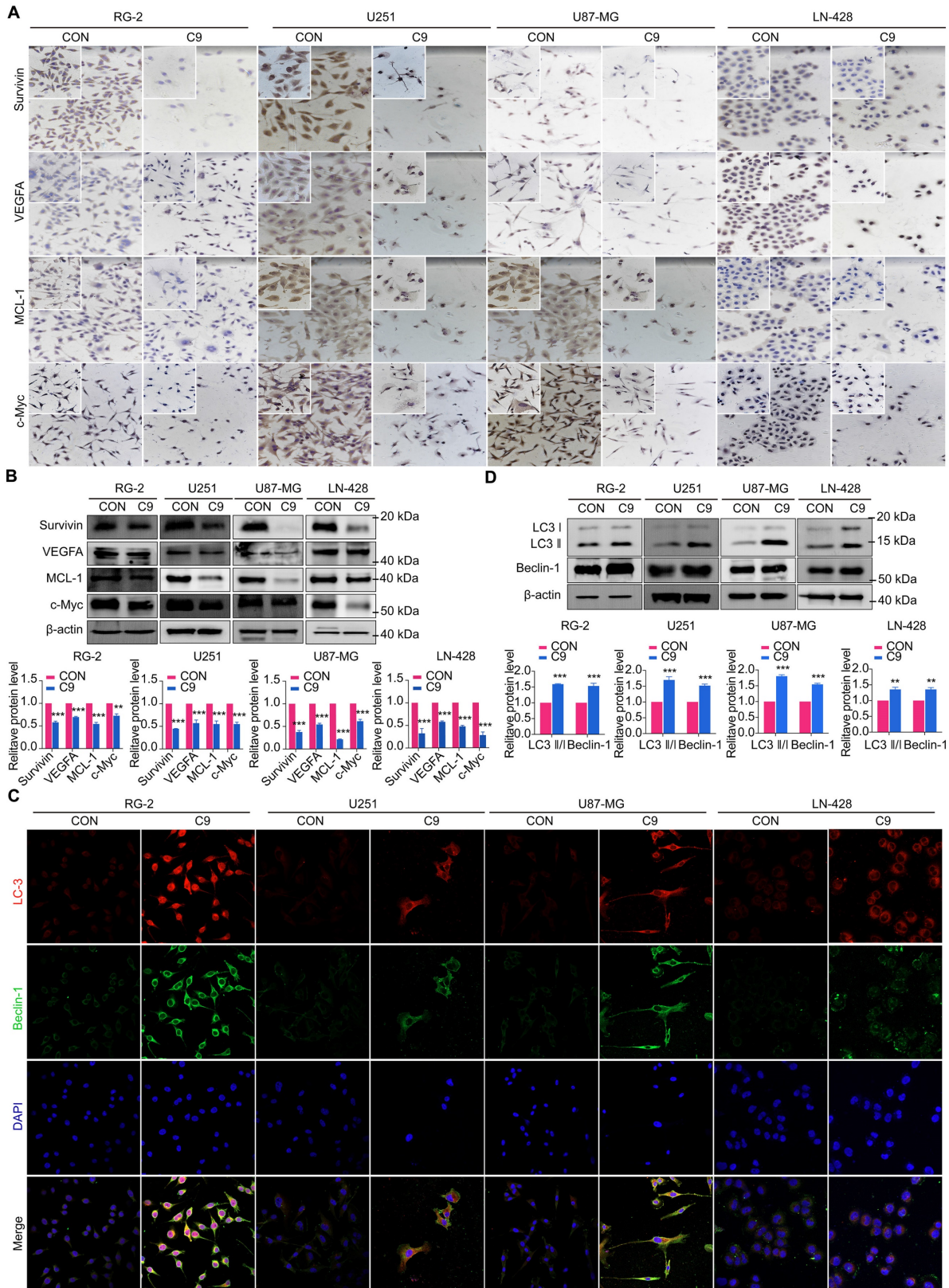


Figure 6. Examinations of MCL-1, Survivin, VEGFA, c-Myc, LC3 II/I and Beclin-1 expression in U251, U87-MG, LN-428, and RG-2 cells without (CON) and with (C9) HUC-MSCs supernatants treatments for 48 h. **(A)** ICC examination ($\times 20$ and $\times 40$) and **(B)** Western blot analyses of MCL-1, Survivin, VEGFA, and c-Myc. β -actin was used as a qualitative and quantitative control. **(C)** IF experiments were performed by laser confocal microscopy ($\times 20$) to examine the expression of the autophagy-related proteins LC3 II/I and Beclin-1. **(D)** Western Blot analyses of LC3 II/I and Beclin-1. β -actin was used as a qualitative and quantitative control. CON, 0 mg/ml HUC-MSCs supernatants; C9, 9 mg/ml HUC-MSCs supernatants. * $P < 0.05$, ** $P < 0.01$ and *** $P < 0.001$ vs CON group; the error bars, the mean \pm standard deviation.

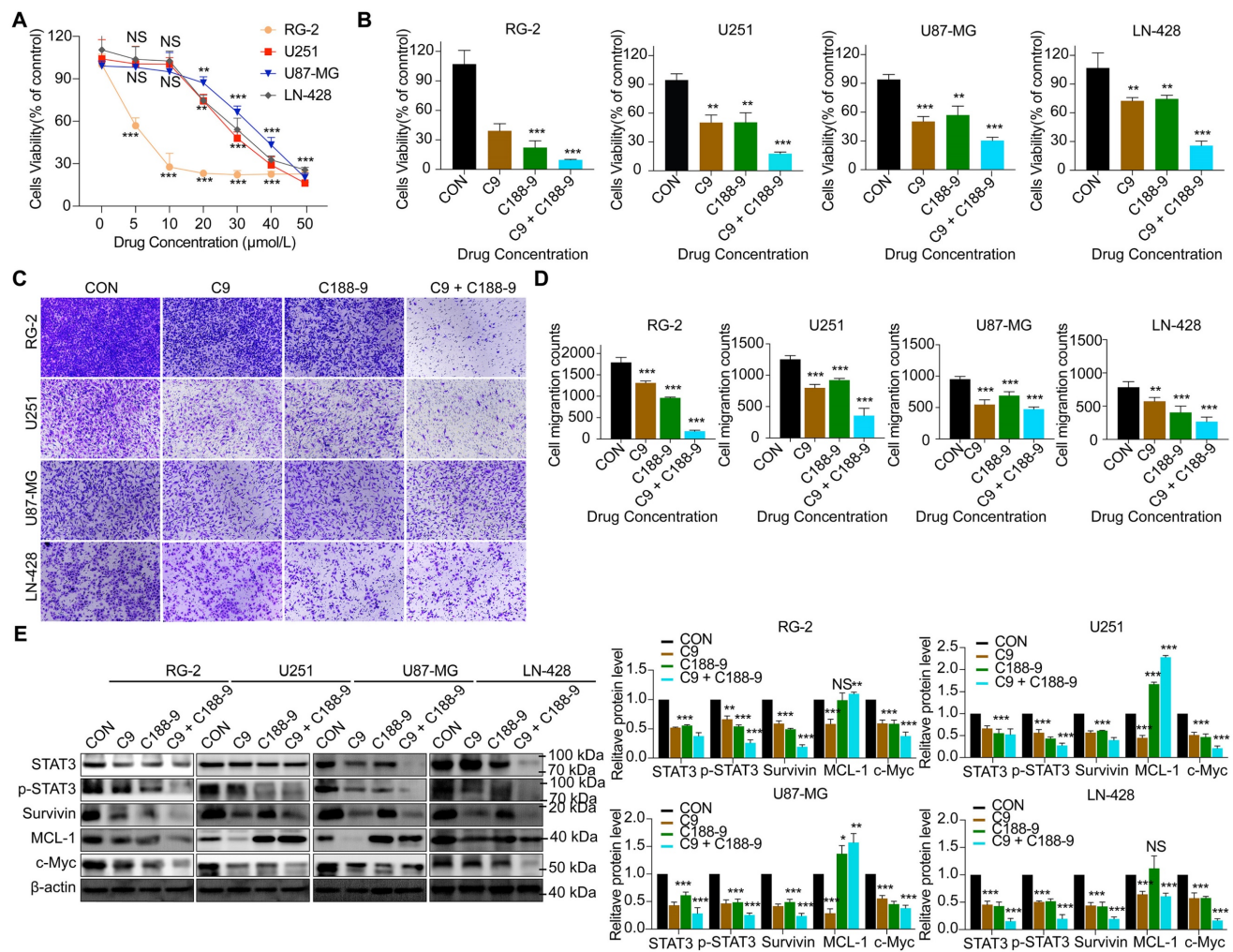


Figure 7. Alterations in STAT3 signaling pathway after 48 h of STAT3 inhibitor C188-9 applied to U251, U87-MG, LN-428, and RG-2 cells. **(A)** CCK-8 assays showing the effect of C188-9 in U251, U87-MG, LN-428, and RG-2 cells. **(B)** CCK-8 assays showing the effect of HUC-MSCs supernatants or/and C188-9 in U251, U87-MG, LN-428, and RG-2 cells. **(C)** Transwell Migration assay. **(D)** Four GBM cell lines were statistically analysed for migration. **(E)** Western Blot analyses of STAT3/p-STAT3 and downstream related proteins Survivin, MCL-1, and c-Myc expression. β-actin was used as a qualitative and quantitative control. CON, Blank control group; C9, 9 mg/ml HUC-MSCs supernatants; C188-9, N-(1',2'-Dihydroxy-1,2'-binaphthalen-4'-yl)-4-methoxybenzenesulfonamide; STAT3 inhibitor; **P* < 0.05, ***P* < 0.01 and ****P* < 0.001 vs CON group; the error bars, the mean ± standard deviation.

HUC-MSCs supernatants inhibit GBM cell proliferation and migration in a STAT3-dependent manner

To determine whether HUC-MSCs supernatants inhibit GBM cells' proliferation and migration in a STAT3-dependent manner. C188-9 inhibited the STAT3 gene in GBM cells, so we used HUC-MSCs supernatants to treat them. From the CCK-8 results, we observed that C188-9 was maintained for 48 h, and U251, U87-MG, LN-428, and RG-2 cells showed concentration-dependent. On balance, we chose 20 μmol/L as the effective concentration (Fig. 7A). In addition, from the CCK-8 results, it was observed that although single HUC-MSCs supernatants inhibited the proliferation and migration of U251 (47.4 ± 11.1%) (*P* < 0.01), U87-MG (50.0 ± 5.5%) (*P* < 0.001), LN-428 (28.1 ± 4.3%) (*P* < 0.01), and RG-2 (63.7 ± 13.7%) (*P* < 0.001) cells, the simultaneous action of HUC-MSCs

supernatants and C188-8 further inhibited their proliferation and migration (Fig. 7B). That is to say, HUC-MSCs supernatants to treat U251, U87-MG, LN-428, and RG-2 cells, whose STAT3 gene was inhibited by STAT3 inhibitor (C188-9). U251 (82.4 ± 2.8%) (*P* < 0.001), U87-MG (67.6 ± 6.8%) (*P* < 0.001), LN-428 (71.5 ± 9.6%) (*P* < 0.001), and RG-2 (90.3 ± 0.8%) (*P* < 0.001) cells proliferation was further inhibited by HUC-MSCs supernatants (Fig. 7B). Transwell migration assays also showed the same results, especially that HUC-MSCs supernatants or/and C188-9 most significantly inhibited the migration of RG-2 cells (Fig. 7C and D). Western Blot results showed that HUC-MSCs supernatants treat U251, U87-MG, LN-428, and RG-2 cells, whose STAT3 gene was inhibited by STAT3 inhibitor (C188-9). STAT3/p-STAT3 experiments in U251 (53.5%/72.3%), U87-MG (71.6%/74.3%), LN-428 (84.6%/80.3%), and RG-2 (62.3%/74.0%) cells were further inhibited by

HUC-MSCs supernatants (Fig. 7E). The expression of STAT3 downstream proteins, Survivin and c-Myc, were also further suppressed in U251 (60.3%/78.0%), U87-MG (77.3%/58.1%), LN-428 (80.6%/83.3%), and RG-2 (80.6%/74.3%) cells. It is worth noting that MCL-1 does not seem to be inhibited by C188-1, and even further promotes the expression of MCL-1. There is no relevant report in the previous literature. We think this may be related to the domain of C188-9 targeting GBM cells, we identified C188-9 as a potent small-molecule that targets the pY peptide-binding site in the SH2 domain of STAT3 [34, 35]. That is, disruption of the pY peptide-binding site in the SH2 region of STAT3 in GBM cells did not affect MCL-1 expression. In summary, HUC-MSCs supernatants inhibit GBM cell proliferation and migration in a STAT3-dependent manner.

Discussion

GBM in gliomas is rapidly growing, aggressive, difficult to detect, has a poor prognosis, a high recurrence rate, and is radiotherapy insensitive [40, 41]. Given that many anti-GBM drugs, at high doses, cause significant toxicity and BBB obstruction in the brain and/or body [42]. The presence of these barriers makes it difficult for many drugs to achieve the desired therapeutic efficacy. As a result, a more effective strategy for treating GBM to supplement or replace existing regimens is urgently needed. HUC-MSCs inhibit tumor growth by secreting relevant cytokines on their own. Studies have shown that HUC-MSCs can induce apoptosis and promote benign progression in oesophageal, ovarian, and leukemia cancer cells [18-20]. However, limitations in delivery and risks of instability in humans are both concerns for HUC-MSCs as cell therapy [19, 43]. HUC-MSCs supernatants, which contain extracellular vesicles and released bioactive molecules, are a viable cell-free therapy alternative [44]. Its activity has the potential to significantly alter neighboring cells' key cellular functions such as survival, apoptosis, maturation, and differentiation [45]. Furthermore, it retains the properties of HUC-MSCs, such as the ability to cross the BBB and tumor propensity. Therefore, in our study, we extracted the supernatant of HUC-MSCs for the treatment of GBM cells. We found that HUC-MSCs supernatants can be purified and freeze-dried into a lyophilized powder for large-scale production, easier storage, and long-term stability of biological activity.

Although previous research has suggested that the immunosuppressive and antitumor effects induced by MSCs on tumor cellular metabolism may be the result of direct cell-cell interactions [46, 47], there has been little investigation into extracting the

supernatant of HUC-MSCs at different times to resist GBM. Our study showed that the HUC-MSCs supernatant was effective and feasible for tumor suppression of GBM cells. We found that the HUC-MSCs supernatants inhibited the proliferation of GBM cells to varying degrees. It is unidentified whether the drug concentration of HUC-MSCs supernatants is hindered by incubation time and FBS. To address these issues, we used two approaches to collect HUC-MSCs supernatants (Fig. 8) and incubated GBM cells at various concentrations and times (Table 1). According to the CCK-8 results, HUC-MSCs supernatants inhibited the growth of GBM cells in a concentration-dependent but not time-dependent manner (Fig. 1A and B). Considered collectively, we used H-DMEM containing 10% FBS for 48 h, we then replaced H-DMEM without FBS to continue incubation for 24 h before collecting 9 mg/ml HUC-MSCs supernatants as the effective concentration for subsequent experiments (Fig. 1C). HUC-MSCs supernatants' inhibition of GBM cells could not be separated from changes in GBM cell apoptosis. HUC-MSCs supernatants were found to affect the proliferation and apoptosis of these four GBM cells in multiple experiments. Our data clearly demonstrated that HUC-MSCs supernatants inhibited GBM cell proliferation while also promoting apoptosis. Among them, rat RG-2 cells were the most sensitive, followed by LN-428 and U87-MG, and U251 was the least sensitive. Changes in the cell cycle are also important in the inhibition of GBM cells by HUC-MSC supernatants. Cyclins and cyclin-dependent protein kinases (CDKs) have been shown in studies to play an important regulatory role in cell cycle progression [48]. Cyclin A2, CDK2, Cyclin D1, and CDK4 are essential to cell cycle regulatory proteins. Cyclin A2 and CDK2 were significantly downregulated in RG-2, U251, and U87-MG cells by HUC-MSC supernatants, whereas Cyclin D1 and CDK4 were downregulated in LN-428 cells (Fig. 2B). Given that MSCs can gravitate to tumor sites and inhibit tumor cell growth [49]. With Transwell assays, we found that HUC-MSCs could converge towards GBM cells *in vitro*, providing a robust scientific foundation for *in vivo* experiments on HUC-MSCs targeting GBM (Fig. 2C).

To explore the molecular mechanisms influenced by HUC-MSCs supernatant, we glanced into the role of the IL-6/JAK2/STAT3 signaling pathway in the inhibition of GBM cell growth by HUC-MSCs supernatants. STAT3 proteins suppress antitumor immunity and accelerate tumor progression. STAT3 activation has been observed in many human cancers, including breast, melanoma, and thyroid cancer [50, 51]. Evidence points to STAT3 playing a critical role in

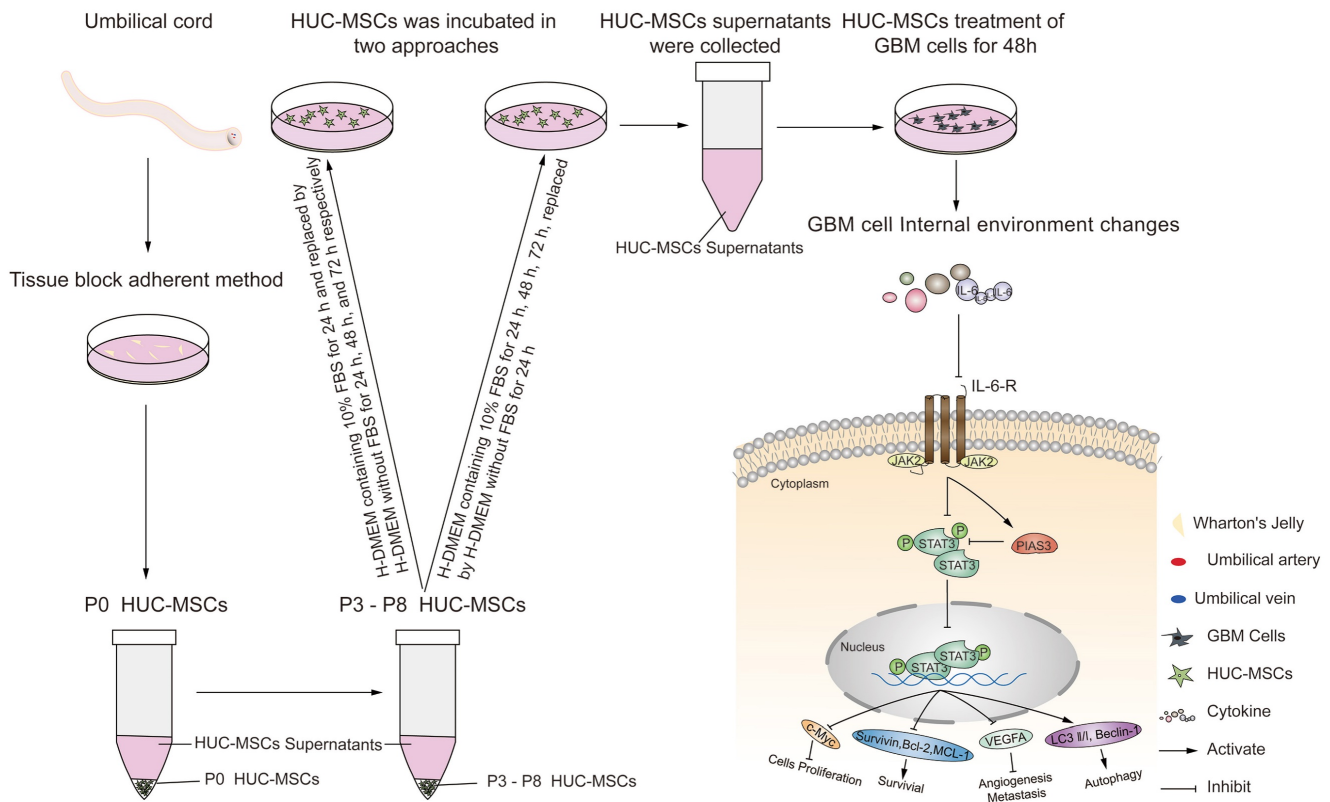


Figure 8. Schematic diagram.

GBM development and progression [52], and its transcriptional activation is regulated by IL-6-mediated JAK2 [27]. STAT3 is an oncogenic transcription factor whose structural and persistent activation of its proteins is highly regulated. STAT3 bound to the promoters of target genes in the nucleus, inducing transcription of genes for cell proliferation (such as cyclin D1, CDK2, and c-Myc), survival (such as MCL-1, Bcl-2, and survivin), angiogenesis-promoting (such as VEGFA) and invasiveness and/or metastasis (such as MMPs) (Fig. 8) [31, 53]. STAT3 signaling has been linked to apoptosis and autophagy in cancer cells [30, 51]. For this reason, it was speculated that the biological consequences of STAT3 inactivation could be mediated by HUC-MSCs supernatants. Using Western Blot and ICC analysis, this study revealed that HUC-MSCs supernatants suppressed the expression of STAT3-regulated proteins IL-6 and JAK2, thereby downregulating STAT3 and p-STAT3 expressions in GBM cells (Fig. 5). Furthermore, the expressions of STAT3 signaling pathway downstream of cellular proliferation-related proteins c-Myc, survival-related proteins MCL-1, Bcl-2 and survivin, and angiogenesis-promoting proteins VEGFA were also observed. From our experimental results, the expression of Survivin, MCL-1, Bcl-2, VEGFA, and c-Myc in GBM cells has been down-regulated in the presence of HUC-MSCs

supernatants (Fig. 6A and B). These observations suggested that the IL-6/JAK2/STAT3 signaling pathway in GBM cells was blocked by HUC-MSCs supernatants. To validate our findings, we used C188-9 to inhibit STAT3 gene expression and found that HUC-MSCs supernatants inhibit the proliferation and migration of GBM cells in a STAT3-dependent manner (Fig. 7E). This finding raises the possibility that HUC-MSCs supernatants is responsible for inhibiting the IL-6/JAK2/STAT3 signaling pathway in GBM cells.

In order to inhibit STAT3 signaling in GBM cells. Subsequently, we sought inhibitors upstream of STAT3, PIAS3, which is one of the most important inhibitors of the STAT3 signaling pathway [54]. PIAS3 blocks STAT3 activity and thus STAT3-mediated activation of downstream genes [54]. PIAS3 is upregulated to inactivate STAT3, promoting apoptosis and autophagy in tumor cells. We used Western blot to determine the effect of PIAS3 by HUC-MSCs supernatants in GBM cells. The results showed a positive correlation between PIAS3 and the concentration of HUC-MSCs supernatants (Fig. 5). This provides evidence that PIAS3 plays an important role in regulating the STAT3 signaling pathway in GBM cells. To further confirm the role of PIAS3, we used ICC assays to determine that PIAS3 inhibited the STAT3 signaling pathway in GBM cells pretreated

with HUC-MSCs supernatants as described above. The present study showed that PIAS3, an upstream inhibitor of the STAT3 signaling pathway, is one of the mechanisms by which HUC-MSCs supernatants inhibit tumor cells. Thus, HUC-MSCs-induced transactivation of the STAT3 signaling pathway may be a potential therapeutic strategy for GBM cells. It should be noted that the degree of STAT3 signaling pathway inhibition varied in different GBM cells, especially in U87-MG cells that were sub-sensitive to HUC-MSCs supernatants. This may be because HUC-MSCs supernatants are involved in antitumor mechanisms differently in U87-MG cells, and further experiments are needed to investigate these issues more fully.

Autophagy is involved in several pathophysiological regulatory processes in humans [55]. So far, no report has been available concerning the status of autophagy and its relevance to HUC-MSCs supernatants' sensitivity in GBM cells either *in vitro* or *in vivo*. Some studies have shown an important relationship between STAT3 signaling in apoptosis and autophagy in tumor cells [19, 54, 56]. We examined autophagy signaling downstream of the STAT3 signaling pathway, such as Beclin-1 and LC3 protein expressions, in GBM cells by Western Blot combined with laser confocal microscopy. The results suggested that Beclin-1 expression was upregulated by HUC-MSCs supernatants and LC3 I was converted to LC3 II in response to HUC-MSCs supernatants in GBM cells (Fig. 6C and D). Thus, the STAT3 signaling pathway promoted autophagy and apoptosis in GBM cells to enhance the therapeutic effect of GBM cells.

Taken together, the results of this study highlight that although we understand how HUC-MSCs supernatant and GBM cells interact, there are still many questions and obstacles on how this could be used to develop targeted therapies for GBM cells.

Conclusion

HUC-MSCs supernatants had a pernicious effect on GBM. It inhibited the proliferation, migration, and invasion of GBM cells, promoting cell apoptosis and negatively regulating the IL-6/JAK2/STAT3 signaling pathway, thereby improving the therapeutic efficacy of GBM.

Abbreviations

GBM: glioblastoma; HUC-MSCs: human umbilical cord mesenchymal stem cells; GSCs: glioblastoma stem cells; CNS: the central nervous system; LGG: low-grade gliomas; HGG: high-grade gliomas; BBB: blood-brain barrier; TMZ: temozolomide; pY: phosphotyrosine; SH: Src-homology; STAT: Signal

transducer and activator of transcription; PIAS3: Protein inhibitor of activated STAT3; TUNEL: Terminal Deoxynucleotidyl Transferase dUTP Nick End Labeling; PI: propidium iodide; ICC: Immunocytochemical Staining; IF: Triple Immunofluorescence Staining; SDS-PAGE: sodium dodecylsulfate-polyacrylamide gel electrophoresis; SD: standard deviation; CDKs: cyclin-dependent protein kinases; MMPs: matrix metalloproteinases.

Acknowledgments

This work was supported by National Natural Science Foundation of China (82260489), The Shaanxi Science and Technology Department Project (2022JQ-931), and Scientific Research Division of Yan'an University (YCX2021086). The funders had no roles in the design of the study, data collection, analysis and interpretation, or decision to write and publish the work.

Author contributions

Conceptualization: Jing Zhang, Yufu Zhang; Methodology: Mingming Wang, Yuna Jia, Haiyan Shi, Yunqing Zhang; Validation: Mingming Wang, Yusi Liu, Jing He, Xiangrong Xu; Formal analysis: Mingming Wang, Yusi Liu, Min Liu; All authors have read and agreed to the published version of the manuscript.

Ethical approval

The study was approved by the Biomedical Ethics Committee of the Medical School of Yan'an University.

Consent to participate

Written informed consents for the use of Umbilical cord tissues samples for scientific purposes were obtained for all individual participants included in the study.

Competing Interests

The authors have declared that no competing interest exists.

References

1. Liu K, Jiang L, Shi Y, et al. Hypoxia-induced GLT8D1 promotes glioma stem cell maintenance by inhibiting CD133 degradation through N-linked glycosylation. *Cell Death Differ.* 2022; 29: 1834-1849.
2. Liu K, Pu J, Nie Z, et al. Ivacaftor Inhibits Glioblastoma Stem Cell Maintenance and Tumor Progression. *Front Cell Dev Biol.* 2021; 9: 678209.
3. Louis DN, Perry A, Wesseling P, et al. The 2021 WHO Classification of Tumors of the Central Nervous System: a summary. *Neuro Oncol.* 2021; 23: 1231-1251.
4. Yang K, Wu Z, Zhang H, et al. Glioma targeted therapy: insight into future of molecular approaches. *Mol Cancer.* 2022; 21: 39.
5. Ostrom QT, Cioffi G, Gittleman H, et al. CBTRUS Statistical Report: Primary Brain and Other Central Nervous System Tumors Diagnosed in the United States in 2012-2016. *Neuro Oncol.* 2019; 21: 1-100.
6. Weller M, Le Rhun E. How did lomustine become standard of care in recurrent glioblastoma? *Cancer Treat Rev.* 2020; 87: 102029.
7. Tomiyama A, Ichimura K. Signal transduction pathways and resistance to targeted therapies in glioma. *Semin Cancer Biol.* 2019; 58: 118-129.

8. Agarwal S, Sane R, Oberoi R, et al. Delivery of molecularly targeted therapy to malignant glioma, a disease of the whole brain. *Expert Rev Mol Med*. 2011; 13: e17.
9. Groothuis DR. The blood-brain and blood-tumor barriers: a review of strategies for increasing drug delivery. *Neuro-oncology* vol. 2000; 2: 45-59.
10. Chacko AM, Li C, Pryma DA, et al. Targeted delivery of antibody-based therapeutic and imaging agents to CNS tumors: crossing the blood-brain barrier divide. *Expert Opin Drug Deliv*. 2013; 10: 907-926.
11. Bauer HC, Krizbai IA, Bauer H, et al. "You Shall Not Pass"-tight junctions of the blood brain barrier. *Front Neurosci*. 2014; 8: 392.
12. Zhan C, Lu W. The blood-brain/tumor barriers: challenges and chances for malignant gliomas targeted drug delivery. *Curr Pharm Biotechnol*. 2012; 13: 2380-7.
13. Liu WH, Song FQ, Ren LN, et al. The multiple functional roles of mesenchymal stem cells in participating in treating liver diseases. *J Cell Mol Med*. 2015; 19: 511-520.
14. Zhang LT, Peng XB, Fang XQ, et al. Human umbilical cord mesenchymal stem cells inhibit proliferation of hepatic stellate cells *in vitro*. *Int J Mol Med*. 2018; 41: 2545-2552.
15. Secunda R, Vennila R, Mohanashankar AM, et al. Isolation, expansion and characterisation of mesenchymal stem cells from human bone marrow, adipose tissue, umbilical cord blood and matrix: a comparative study. *Cytotechnology*. 2015; 67: 793-807.
16. Wu KH, Liu YL, Zhou B, et al. Cellular therapy and myocardial tissue engineering: the role of adult stem and progenitor cells. *Eur J Cardiothorac Surg*. 2006; 30: 770-781.
17. Jo CH, Kim OS, Park EY, et al. Fetal mesenchymal stem cells derived from human umbilical cord sustain primitive characteristics during extensive expansion. *Cell Tissue Res*. 2008; 334: 423-433.
18. Wang Y, Fan H, Zhou B, et al. Fusion of human umbilical cord mesenchymal stem cells with esophageal carcinoma cells inhibits the tumorigenicity of esophageal carcinoma cells. *Int J Oncol*. 2012; 40: 370-377.
19. Melzer C, von der Ohe J, Hass R. MSC stimulate ovarian tumor growth during intercellular communication but reduce tumorigenicity after fusion with ovarian cancer cells. *Cell Commun Signal*. 2018; 16: 67.
20. Xie Q, Liu R, Jiang J, et al. What is the impact of human umbilical cord mesenchymal stem cell transplantation on clinical treatment? *Stem Cell Res Ther*. 2020; 11: 519.
21. Ma S, Liang S, Jiao H, et al. Human umbilical cord mesenchymal stem cells inhibit C6 glioma growth via secretion of dickkopf-1 (DKK1). *Mol Cell Biochem*. 2014; 385: 277-286.
22. Zou S, Tong Q, Liu B, et al. Targeting STAT3 in Cancer Immunotherapy. *Mol Cancer*. 2020; 19:145.
23. Darnell JE, Kerr IM, Stark GR. Jak-STAT pathways and transcriptional activation in response to IFNs and other extracellular signaling proteins. *Science (New York, N.Y.)*. 1994; 264: 1415-1421.
24. Hanlon MM, Rakovich T, Cunningham CC, et al. STAT3 Mediates the Differential Effects of Oncostatin M and TNF α on RA Synovial Fibroblast and Endothelial Cell Function. *Front Immunol*. 2019; 10: 2056.
25. Rawlings JS, Rosler KM, Harrison DA. The JAK/STAT signaling pathway. *J Cell Sci*. 2004; 117:1281-1283.
26. Levy DE, Darnell JE. Stats: transcriptional control and biological impact. *Nat Rev Mol Cell Biol*. 2002; 3: 651-662.
27. Zhao J, Jiang Y, Zhang H, et al. The SRSF1/circATP5B/miR-185-5p/HOXB5 feedback loop regulates the proliferation of glioma stem cells via the IL6-mediated JAK2/STAT3 signaling pathway. *J Exp Clin Cancer Res*. 2021; 40: 134.
28. Hu C, Xia R, Zhang X, et al. circFARP1 enables cancer-associated fibroblasts to promote gemcitabine resistance in pancreatic cancer via the LIF/STAT3 axis. *Mol Cancer*. 2022; 21: 24.
29. Lakkaraju AK, van der Goot FG. Calnexin controls the STAT3-mediated transcriptional response to EGF. *Mol Cell*. 2013; 51: 386-396.
30. Chung CD, Liao J, Liu B, et al. Specific inhibition of Stat3 signal transduction by PIAS3. *Science*. 1997; 278: 1803-1805.
31. Johnson DE, O'Keefe RA, Grandis JR. Targeting the IL-6/JAK/STAT3 signalling axis in cancer. *Nat Rev Clin Oncol*. 2018; 15: 234-248.
32. Susman S, Pirlog R, Leucuța D, et al. The role of p-Stat3 Y705 immunohistochemistry in glioblastoma prognosis. *Diagn Pathol*. 2019; 14: 124.
33. Xue H, Yuan G, Guo X, et al. A novel tumor-promoting mechanism of IL6 and the therapeutic efficacy of tocilizumab: Hypoxia-induced IL6 is a potent autophagy initiator in glioblastoma via the p-STAT3-MIR155-3p-CREBRF pathway. *Autophagy*. 2016; 12: 1129-1152.
34. Xu X, Kasembeli MM, Jiang X, et al. Chemical probes that competitively and selectively inhibit Stat3 activation. *PLoS One*. 2009; 4: e4783.
35. Redell MS, Ruiz MJ, Alonzo TA, et al. Stat3 signaling in acute myeloid leukemia: ligand-dependent and -independent activation and induction of apoptosis by a novel small-molecule Stat3 inhibitor. *Blood*. 2011; 117: 5701-5709.
36. Cao S, Guo J, He Y, et al. Nano-loaded human umbilical cord mesenchymal stem cells as targeted carriers of doxorubicin for breast cancer therapy, *Artif Cells Nanomed Biotechnol*. 2018; 46: 642-652.
37. Sherry MM, Reeves A, Wu JK, et al. STAT3 is required for proliferation and maintenance of multipotency in glioblastoma stem cells. *Stem Cells*. 2009; 27: 2383-2392.
38. Liu Y, Song X, Wu M, et al. Synergistic Effects of Resveratrol and Temozolomide Against Glioblastoma Cells: Underlying Mechanism and Therapeutic Implications. *Cancer Manag Res*. 2020; 12: 8341-8354.
39. Zou S, Tong Q, Liu B, et al. Targeting STAT3 in Cancer Immunotherapy. *Mol Cancer*. 2020; 19: 145.
40. Purow B, Schiff D. Advances in the genetics of glioblastoma: are we reaching critical mass? *Nat Rev Neurol*. 2009; 5: 419-426.
41. Wen PY, Weller M, Lee EQ, et al. Glioblastoma in adults: a Society for Neuro-Oncology (SNO) and European Society of Neuro-Oncology (EANO) consensus review on current management and future directions. *Neuro-oncology*. 2020; 22: 1073-1113.
42. Sarkaria JN, Hu LS, Parney IF, et al. Is the blood-brain barrier really disrupted in all glioblastomas? A critical assessment of existing clinical data. *Neuro-oncology*. 2018; 20: 184-191.
43. Lou G, Chen Z, Zheng M, et al. Mesenchymal stem cell-derived exosomes as a new therapeutic strategy for liver diseases. *Exp Mol Med*. 2017; 49(6): e346.
44. Cao J, Wang B, Tang T, et al. Three-dimensional culture of MSCs produces exosomes with improved yield and enhanced therapeutic efficacy for cisplatin-induced acute kidney injury. *Stem Cell Res Ther*. 2020; 11(1): 206.
45. Whiteside TL. Exosome and mesenchymal stem cell cross-talk in the tumor microenvironment. *Semin Immunol*. 2018; 35: 69-79.
46. Meisel R, Zibert A, Laryea M, et al. Human bone marrow stromal cells inhibit allogeneic T-cell responses by indoleamine 2,3-dioxygenase-mediated tryptophan degradation. *Blood*. 2004; 103: 4619-4621.
47. Camorani S, Hill BS, Fontanella R, et al. Inhibition of Bone Marrow-Derived Mesenchymal Stem Cells Homing Towards Triple-Negative Breast Cancer Microenvironment Using an Anti-PDGFR β Aptamer. *Theranostics*. 2017; 7: 3595-3607.
48. Bertoni G. Cell Cycle Regulation by Chlamydomonas Cyclin-Dependent Protein Kinases, *Plant Cell*. 2018; 30: 271.
49. Qiao L, Xu Z, Zhao T, et al. Suppression of tumorigenesis by human mesenchymal stem cells in a hepatoma model. *Cell Res*. 2008; 18: 500-507.
50. Bromberg J. Stat proteins and oncogenesis. *J Clin Invest*. 2002; 109: 1139-1142.
51. Weber A, Borghouts C, Delis N, et al. Inhibition of Stat3 by peptide aptamer rS3-PA enhances growth suppressive effects of irinotecan on colorectal cancer cells. *Horm Mol Biol Clin Investig*. 2012; 10: 273-279.
52. Bian Z, Ji W, Xu B, et al. Noncoding RNAs involved in the STAT3 pathway in glioma. *Cancer Cell Int*. 2021; 21: 445.
53. Bournazou E, Bromberg J. Targeting the tumor microenvironment: JAK-STAT3 signaling. *JAKSTAT*. 2013; 2: e23828.
54. You L, Wang Z, Li H, et al. The role of STAT3 in autophagy. *Autophagy*. 2015; 11: 729-739.
55. Zhang XJ, Chen S, Huang KX, Le WD. Why should autophagic flux be assessed? *Acta Pharmacol Sin*. 2013; 34: 595-599.
56. Zanutto-Filho A, Braganhol E, Klafke K, et al. Autophagy inhibition improves the efficacy of curcumin/temozolomide combination therapy in glioblastomas. *Cancer Lett*. 2015; 358(2): 220-231.